Engineering

Electrical Engineering fields

Okayama University *Year* 1993

A waveguide type power divider/combiner of double-ladder multiple-port structure

Atsushi Sanada
Okayama University

Kiyoshi Fukui
Okayama University

Shigeji Nogi
Okayama University

A Waveguide Type Power Divider/Combiner of Double-Ladder Multiple-Port Structure

Atsushi Sanada, *Student Member, IEEE,* Kiyoshi Fukui, *Member, IEEE,* and Shigeji Nogi, *Member, IEEE*

Abstract— **We propose a waveguide type microwave power divider/combiner of double-ladder multiple-port structure which is advantageous for its very low insertion loss and high power capability. Analysis based on equivalent circuits gives the design formula for perfect power dividing/combining. Numerical analysis gives optimal design parameters for broadband characteristics both of the divider and of the combiner. Analyses of power flows in the divider structure and isolation characteristic are given. Operation characteristics of divider-combiner system and the effect of phase deviation in combiner input signals on the combining efficiency are also discussed. Experiments showed good performances in accordance with the theory: The −0.5 dB relative bandwidths of four-, eight- and twelve-way dividers were as large as 0.5, 0.38, and 0.38, respectively. For four- and eight-way divider-combiner systems, relative bandwidths were 0.22 and 0.13, respectively, both with insertion loss of less than 0.1 dB.**

I. Introduction

METHODS for combining output powers from a number of solid-state devices have been extensively studied in order to obtain higher and higher output power for use in satellite communication and satellite broadcasting [1]–[13]. Typical power combining techniques consist of three stages: dividing of a signal to be amplified, amplification of each divided signal and combining of the amplified signals. To obtain higher output power and wideband characteristics, it is required to develop multiple-port power divider/combiner's of low insertion loss, high handling power and wideband characteristics.

Power divider/combiner's can be classified into the nonresonant type such as 3-dB hybrids and radial-line dividers [14], [3]–[9], and the resonant type which uses a cylindrical cavity or a waveguide cavity [10]–[13]. A multiple-port corporate structure using 3-dB hybrids can readily provide wideband characteristics and high isolations but has considerable insertion loss when the number of ports increases. On the other hand, the resonant type, in general, has a high combining efficiency and permits N-way dividing/combining while it is inherently of narrow band. Radial-line dividers have broader frequency characteristics compared with the resonant type.

In the previous paper [13], the authors proposed a microwave power divider/combiner with a multiple-port ladder structure which is essentially a rectangular waveguide cavity having an array of coaxial probe-pairs placed symmetrically with the guide axis and an input/output iris. Although this configuration resembles a resonant type, it was shown that fairly broadband characteristic can be realized as long as it does not have so many coaxial probe-pairs, and that it creates less loss and can handle higher power than those using strip lines. This paper presents a more advanced divider/combiner with double-ladder multiple-port structure. The double-ladder structure refers to the one paired by two same single-ladder structures with no input/output iris but with an input/output coaxial probe between them. Since the divider/combiner is regarded as parallel-running two single-ladder structures, it is expected to be capable of doubling the number of ports without deteriorating its characteristics. This will be of great advantage because the bandwidth of a ladder structure usually decreases with number of ports.

In the following section, an equivalent circuit is introduced and design formulas are given for perfect power dividing/combining. Operation and characteristics of the divider are discussed in Section III. Optimal probe admittance for broadband characteristics is obtained through numerical analysis. By means of analysis of power flows in the structure, physical interpretation of perfect power dividing is given. By treating the divider as a multiple port circuit, S-parameters are derived theoretically and isolation characteristics are discussed. Numerical analysis of frequency characteristics of isolation is also carried out. Section IV is devoted to discussion of combining operation. Analysis of a combiner with phase deviation of input signals is also given. Description of frequency characteristics of divider-combiner systems is followed. Finally, in Section V experiments on the divider/combiner's are carried out and compared with the theory.

II. Design for Perfect Power Dividing/Combining

Fig. 1 shows a double-ladder power divider/combiner. The double-ladder divider/combiner consists of a coaxial input/output probe in the middle of the waveguide and two same ladder structures with N ($2N$ in total) paired coaxial probes placed at both sides of the input/output probe. It is possible for the divider/combiner to divide an input power equally with no reflection loss at the input port, and to combine $4N$ equal-amplitude inputs completely. Fig. 2(a) shows an equivalent circuit of the double-ladder divider. It is assumed in the analysis that only the dominant mode propagates in the waveguide. The circuit represents the right side alone of the divider since the divider is symmetrical with the center probe. $y_p = g_p + jb_p$ and $y_c = g_c + jb_c$ are the admittances of matched probe-pairs and the central probe, respectively, each admittance being normalized by the characteristic admittance

Manuscript received April 21, 1993; revised August 24, 1993.

The authors are with the Department of Electrical & Electronics Engineering, Okayama University, Okayama 700, Japan.

IEEE Log Number 9402367.

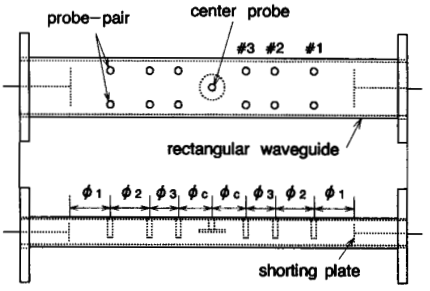

Fig. 1. Divider/combiner with double-ladder structure ($N = 3$).

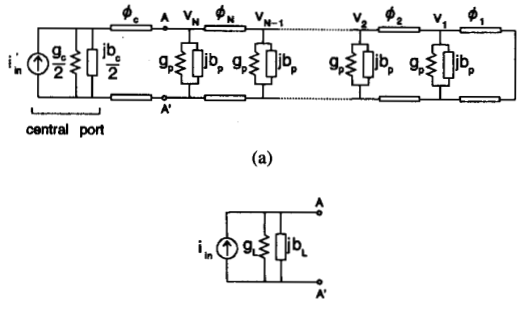

Fig. 2. Equivalent circuit of the divider. (a) Equivalent circuit for the right half of the divider. (b) Simplification of the input part.

Y_0 of the waveguide. ϕ_k's $(1 \le k \le N)$ are electrical lengths between neighboring probe-pairs. The input part is rewritten as a current source $i_\in$ with an internal admittance $y_L = g_L + jb_L$ which is the admittance looking from N-th probe-pair to the left (Fig. 2(b)).

Denoting the current source as $i_{\text{in}} = I_{\text{in}} \exp\{j(\omega_0 t + \psi)\}$ and the voltages of k-th node as $v_k = V_k \exp\{j(\omega_0 t + \varphi_k)\}$ $(1 \le k \le N)$, we can obtain the following circuit equations, (1), shown at the bottom of the page where

$$b_k = \begin{cases} -\cot\phi_k + b_p - \cot\phi_{k+1} & (1 \le k \le N-1) \\ -\cot\phi_k + b_p + b_L & (k = N) \end{cases} \tag{2}$$

$$b_{t,k} = \operatorname{cosec}\phi_k \quad (2 \le k \le N) \tag{3}$$

and

$$\varphi_{m,n} = \varphi_m - \varphi_n. \tag{4}$$

Two conditions must be satisfied so as to divide an input power equally with no reflection loss: 1) The sum of powers provided to each probe-pair, $\sum_k (1/2) g_p Y_0 V_k{}^2$, is equal to the available power of the input current source and 2) all the amplitudes of

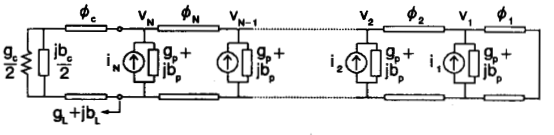

Fig. 3. Equivalent circuit for the right half of the combiner.

the node voltages are equal; i.e., $V_1 = V_2 = \cdots = V_N \equiv V$. Design formulas for perfect power dividing are given under those conditions as

$$g_L = N g_p \tag{5}$$

$$b_L = -\frac{b_p}{2} \tag{6}$$

$$-\cot\phi_k = \begin{cases} -\frac{b_p}{2} & (k = 1) \\ \frac{1}{b_p}\left\{1 - (\frac{b_p}{2})^2 - (k-1)^2 g_p^2\right\} & (2 \le k \le N). \end{cases} \tag{7}$$

When the values of g_p and b_p are specified, those of the load admittance $g_L + jb_L$ and electrical distances $\phi_1 \sim \phi_N$ can be determined.

Fig. 3 shows an equivalent circuit of the combiner. The input from the k-th probe-pair is represented by a current source i_k with an internal admittance equal to $g_p + jb_p$, and an admittance looking from N-th probe-pair to the left is represented by $y_L (= g_L + jb_L)$.

In Fig. 3, let the current source be $i_k = I_k \exp\{j(\omega_0 t + \psi_k)\}$. When all the input powers are equal $(I_1 = I_2 = \cdots = I_N \equiv I)$, the design for perfect power combining in which an output power of the combiner P_{out} is equal to the sum of the available power of each current source $\sum_k {I_k}^2/(8 g_p Y_0)$ are given by the same expression as (5) $\sim$ (7). Thus, the same structure can be used for perfect power dividing and for perfect power combining.

Under the perfect power dividing condition, the phase relations of node voltages are given from (1) by

$$\sin(\varphi_k - \varphi_{k-1}) = (k-1) g_p \sin\phi_k \tag{8}$$

and for perfect power combining, the phase relations of input signals applied to the combiner probe-pairs must be given by

$$\sin(\psi_k - \psi_{k-1}) = -(k-1) g_p \sin\phi_k. \tag{9}$$

These relations must be considered when the divider/combiner is used as a system component.

The design formulas (5) and (6) provide the load admittance $y_L = g_L + jb_L$ looking from the N-th probe-pair, but the design is not unique because y_L depends on the admittance $y_c = g_c + jb_c$ and the distance ϕ_c. Note that the half of the

$$\left.\begin{array}{ll} (g_p + jb_k)V_k + jb_{t,k+1} V_{k+1} e^{j\varphi_{k+1,k}} = 0 & (k = 1) \\ jb_{t,k} V_{k-1} e^{-j\varphi_{k,k-1}} + (g_p + jb_k)V_k + jb_{t,k+1} V_{k+1} e^{j\varphi_{k+1,k}} = 0 & (2 \le k \le N-1) \\ jb_{t,k} V_{k-1} e^{-j\varphi_{k,k-1}} + (g_p + g_L + jb_k)V_k = Y_0^{-1} I_{\text{in}} e^{j(\psi - \varphi_k)} & (k = N), \end{array}\right\} \tag{1}$$

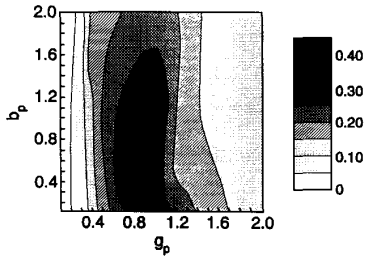

Fig. 4. Dependence of -0.5 dB relative bandwidth on the admittance of the probe pair ($N = 2$).

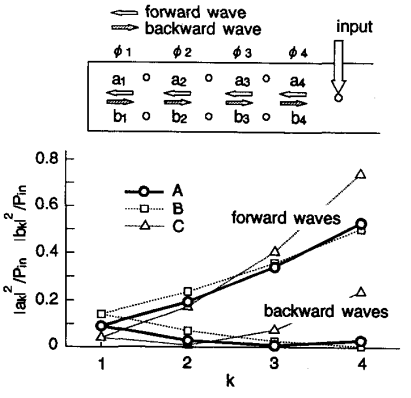

Fig. 5. Forward and backward waves in the structure ($N = 3$). A.. Optimal parameter values: $g_p = 0.5$, $b_p = 0.6$. B. Other parameter values: $g_p = 0.3$, $b_p = 0.3$. C. Other parameter values: $g_p = 1.2$, $b_p = 0.8$.

admittance of center probe $y_c/2$ should be matched to y_L with the distance ϕ_c:

$$y_c = 2\frac{y_L - j\tan\phi_c}{1 - jy_L\tan\phi_c}. \tag{10}$$

It is desirable that the ϕ_c is chosen as short as possible so as to minimize the frequency dependence of y_L, though this may be limited by the size of the connector of the input/output port.

III. Analysis on the Characteristics of the Divider

A. Broadband Power Dividing

Numerical analysis was carried out on the frequency characteristics of the double-ladder divider designed at $\omega_0/2\pi = f_0 = 9.0$ GHz, in which no frequency dependence of $g_p + jb_p$ was assumed (A typical data is shown in Fig. 9 in Section V). ϕ_c is chosen to be $\pi/2$ and y_c is determined so as to satisfy (10) at the frequency f_0.

Frequency characteristics of the divider depend on the admittance of the probe-pair $g_p + jb_p$ because (5) $\sim$ (7) are used for the design. In order to estimate broadband characteristics, we consider the band in which transmission of more than -0.5 dB is obtained, and define -0.5 dB relative bandwidth as the ratio of the band to f_0. Its dependence on g_p and b_p was calculated and a result is shown in Fig. 4. Table I-A shows the maximal -0.5 dB-relative bandwidth and the corresponding values of g_p and b_p for $N = 1 \sim 5$ under the limitation of $\phi_k \geq 1.2$ rad ($2 \leq k \leq N$) at 9.0 GHz, which comes from the size of the connectors of the output ports. The maximal bandwidth for each value of N does not have much differences between the design for $b_p > 0$ and that for $b_p < 0$, and decreases with N. Note that wideband characteristics of more than 36% are obtained for dividers with $b_p > 0$. Compared with single-ladder dividers [13] with half number of port-pairs, the bandwidths (BW) is a little wider since the distance of ϕ_c can be shortened in the case of this structure (The BW becomes more than sixteen percent wider for $\phi_c = \pi/2$ while that is a little narrower for $\phi_c = \pi$, compared with single-ladder structures of same N).

TABLE I
Optimal Values of g_p and b_p and Maximal -0.5 dB Relative Bandwidth BW ($\phi_c = \pi/2$). (A) Divider (B) Combiner. (C) Divider-Combiner System.

(a) Divider.

N(number of ports)		1(4)	2(8)	3(12)	4(16)	5(20)
$b_p > 0$	g_p	1.40	1.00	0.50	0.35	0.35
	b_p	0.20	0.10	0.60	0.75	0.65
	relative BW	0.46	0.43	0.43	0.36	0.37
$b_p < 0$	g_p	1.40	0.90	0.50	0.50	0.25
	b_p	-0.10	-0.30	-0.05	-0.05	-0.95
	relative BW	0.45	0.38	0.39	0.27	0.23

(b) Combiner.

N(number of ports)		1(4)	2(8)	3(12)	4(16)	5(20)
$b_p > 0$	g_p	1.40	0.90	0.45	0.50	0.35
	b_p	0.20	0.40	0.30	0.60	0.75
	relative BW	0.46	0.30	0.17	0.12	0.09
$b_p < 0$	g_p	1.40	0.90	0.55	0.45	0.35
	b_p	-0.10	-0.40	-0.20	-0.40	-0.15
	relative BW	0.45	0.24	0.14	0.10	0.09

(c) Divider-combiner system.

N(number of ports)		1(4)	2(8)	3(12)	4(16)	5(20)
$b_p > 0$	g_p	1.40	0.85	0.45	0.30	0.30
	b_p	0.10	0.55	0.20	0.05	0.10
	relative BW	0.39	0.23	0.13	0.07	0.06
$b_p < 0$	g_p	1.40	0.80	0.55	0.35	0.35
	b_p	-0.10	-0.70	-0.10	-0.05	-0.05
	relative BW	0.39	0.17	0.09	0.06	0.05

B. Forward and Backward Waves and Power Flow in the Structure

Let us consider a distribution of forward and backward waves and power flow in the structure. Consider forward and backward waves on the portion ϕ_k (See the top of Fig. 5) and

denote these waves defined at the center of ϕ_k as a_k and b_k, respectively.[1] Powers of these values are given using (7) and (8) by

$$\left.\begin{matrix}|a_k|^2\\|b_k|^2\end{matrix}\right\} = \frac{1}{8}Y_0V^2\left[\{(k-1)g_p \pm 1\}^2 + \left(\frac{b_p}{2}\right)^2\right] \quad (k=1,2,\ldots,N) \tag{11}$$

[15]. Then the power flow is written as

$$|a_k|^2 - |b_k|^2 = \frac{1}{2}(k-1)g_pY_0V^2 \tag{12}$$

$$= (k-1)\frac{P_{\text{in}}}{2N}(k=1,2,\ldots,N). \tag{13}$$

Equation (13) shows that the divider can equally divide an input power P_{in} into $2N$ portions, or, in other words, that the perfect power dividing is realized.

Under the condition of perfect power dividing at the frequency f_0, reflected waves by the probe-pairs and by the shorting plate are cancelled completely at the input port. At a frequency of $f \neq f_0$, the cancellation condition does not hold, so that the transmission efficiency η_{div} is degraded. In such case, the smaller the amount of each reflected wave is, the smaller the degradation of transmission efficiency η_{div} becomes and the broader the bandwidth of the divider is. Fig. 5 shows a power flow distribution of the forward and backward waves in the structure of the divider of $N = 3$ for both the cases of the optimal and of other parameters values. The power of the forward wave $|a_k|^2$ decreases due to successive power providing to probe-pairs. The power incident to the shorting plate passing probe-pair #1 is $1/(8Ng_p)$ times the input power of the divider when $(b_p/2)^2 \ll 1$. In the optimal design for $N = 3$, the power reflected by the shorting plate is about 0.08 relative to the input power, and backward waves between neighboring probe-pairs are much less. On the other hand, the power of forward waves increases with k. Because all the optimal design for $N = 1 \sim 5$ have similar distributions of forward and backward waves, the structure given by the broadband design exhibits a quasi-traveling wave type operation.

C. S-Parameters and Isolation of the Divider

In order to discuss power transmission characteristics between ports of the divider, S-parameters of the divider are calculated. Assume that an input signal is applied to one of the l-th port-pair. If the input signal is represented by a current source $i_{\text{in}} = I_{\text{in}}\exp\{j(\omega_0 t + \psi)\}$ with an internal admittance $(g_p + jb_p)/2$, then an equivalent circuit can be written as in Fig. 6 which is the same as that for the divider except the position of the input current source. Hence circuit equations can be obtained in the same way as (1), from which S-parameters of the divider are given by

$$|S_{kl}|^2 = \begin{cases} \frac{3g_p}{16Ng_l}\prod_{m=l+1}^{N}\left(\frac{g_p}{g_m}+1\right) & (k=1,2,\cdots l-1,\ L) \\ \frac{3g_p}{16Ng_k}\prod_{m=k+1}^{N}\left(\frac{g_p}{g_m}+1\right) & (k=l+1,l+2,\cdots,N-1) \\ \frac{g_p}{8Ng_c} & (k=N) \\ \frac{1}{4N} & (k=0) \\ \frac{1}{16N^2} & (k=1',2',\ldots,N'), \end{cases} \tag{14}$$

where "0" is assigned to the central port. In a discussion based on the equivalent circuit, signal transmissions to both ports of k-th ($k \neq l$) port-pair are identical, so that both are denoted by the same symbol S_{kl} in (14). A signal transmission to another port of the l-th port-pair is denoted as S_{Ll}. Port-pair numbers in the opposite side of the central probe are denoted as $1', 2', \ldots, N'$. g_k is a conductance of the admittance $y_k = g_k + jb_k$ looking from the k-th probe-pair toward the central probe as shown in Fig. 6. y_k is given by

$$y_k = \frac{(y_{k+1} + y_p) + j\tan\phi_{k+1}}{1 + j(y_{k+1} + y_p)\tan\phi_{k+1}} \quad (1 \le k \le N) \tag{15}$$

where,

$$y_{N+1} + y_p = \frac{3g_c}{2} + j\frac{b_c}{2}$$

and ϕ_k is given by (7). Magnitudes of diagonal components of S-matrix are given from unitarity by

$$|S_{ll}|^2 = 1 - 2\sum_{k\neq l}|S_{kl}|^2 - |S_{Ll}|^2 - |S_{0l}|^2 \tag{16}$$

if the divider is assumed to be lossless.

Isolation characteristics can be estimated by the non-diagonal components of S-matrix. Frequency characteristics of the isolation are obtained based on the equivalent circuit shown in Fig. 6. Fig. 7 shows the theoretical results for the divider of $N = 3$ (twelve-way). In the figure, power transmission coefficients which are relatively large when the input signal is applied to port #1a are depicted. The letters "#1" $\sim$ "#3" and "center" in the figure indicate the power transmission to the ports #1 $\sim$ #3 and the central port of the divider, respectively. The power transmission coefficients are smaller than -10 dB around $f_0 = 9.0$ GHz in the case of the divider of $N = 3$, and decreases with increasing number of the ports. Power transmission coefficients to ports on the opposite side of the center probe are very small as compared with those shown in Fig. 7.

The double-ladder structure has a little improvement in isolation characteristics compared with the single-ladder one. Generally speaking, the numerical results shows that magnitudes of the transmission coefficients decrease with the number of the ports.

IV. Analysis on the Operation of the Combiner

Due to reciprocity theorem, operation of a combiner can be known from that of the divider. However, it is actually difficult

[1] The notation b_k is not for a susceptance but for a normal wave variable in this section.

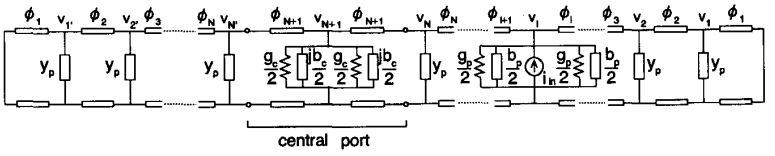

Fig. 6. Equivalent circuit for analysis of isolation.

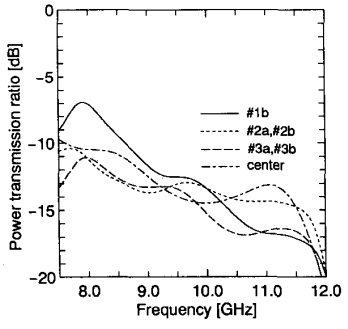

Fig. 7. Isolation characteristics between port #1a and the other ports of the divider/combiner ($N = 3$).

to adjust the amplitudes and the phases of input signals of a combiner to coincide with the corresponding ones when it is used as a divider. Therefore, the operation of the combiner must be discussed separately from that of the divider.

A. Broadband Power Combining

Let us consider $4N$ signals with equal-amplitude and equal-phase and let them feed the combiner through coaxial cables whose electrical lengths Ψ_k are $(\psi_1 - \psi_k + \text{constant})$ for k-th port-pair $(1 \leq k \leq N)$ so as to satisfy the condition of (9) at the frequency $f_0 = 9.0$ GHz $(0 \leq \Psi_k < 2\pi$ is assumed). Under this situation, frequency characteristics of the output power of the combiner are calculated based on the equivalent circuit of Fig. 3. Table I–B shows -0.5 dB relative bandwidths and probe admittances g_p and b_p which give maximal bandwidths for the combiner of $N = 1 \sim 5$. The optimal values of g_p and b_p are similar to those for the divider but the bandwidths are narrower than in the divider except the case $N = 1$. This is partly because the reciprocity between divider and combiner cannot hold except at design frequency, and partly because the dispersion characteristics are different between the connecting coaxial cables and the waveguide of the combiner.

B. Combiner Operation with Input Signals with Phase Deviation

The phase of the input signals to k-th port must satisfy (9) for perfect power combining, and phase deviation from (9) lowers the combining efficiency. The deterioration of the combining efficiency can be analysed as follows.

Let us denote the output port as the 0-th port, the input ports as the i-th port $(1 \leq i \leq 4N)$ and incident waves into the combiner as $\mathbf{a}_T = {}^t[0\ a_1\ \cdots\ a_{4N}]$, output waves as $\mathbf{b}_T = {}^t[b_0\ b_1\ \cdots\ b_{4N}]$. The S-matrix of the combiner can be represented as

$$\mathbf{b}_T = \mathbf{S}\mathbf{a}_T$$

$$\mathbf{S} \equiv \begin{bmatrix} S_{00} & \mathbf{d} \\ {}^t\mathbf{d} & \mathbf{S}' \end{bmatrix} \tag{19}$$

where S_{00} is the reflection coefficient at the output port and $\mathbf{d}$ is the vector whose components are the transmission coefficients between the input ports and the output port. Now let $\mathbf{a}$ be an input wave vector which has the same components as $\mathbf{a}_T$ except the first component is removed: $\mathbf{a} = {}^t[a_1\ a_2\ \cdots\ a_{4N}]$. An arbitrary input wave $\mathbf{a}$ can be expanded using the perfect combining mode $\mathbf{a}_0$ and the independent orthogonal non-combining modes $\mathbf{a}_\nu$'s $(1 \leq \nu \leq 4N - 1)$:

$$\mathbf{a} = \sum_{\nu=0}^{4N-1} \eta_\nu \mathbf{a}_\nu \tag{20}$$

where $\mathbf{a}_\nu$'s $(0 \leq \nu \leq 4N - 1)$ are assumed to be normalized. Because $\mathbf{a}_0$ is the perfect combining mode, $|\mathbf{d} \cdot \mathbf{a}_0| = 1$. Therefore the vector $\mathbf{d}$ is parallel to the conjugate vector $\bar{\mathbf{a}}_0$. Since, on the other hand, $\bar{\mathbf{a}}_0 \cdot \mathbf{a}_\nu = 0$ $(\nu \neq 0)$, we have

$$\mathbf{d} \cdot \mathbf{a}_\nu = 0.$$

Thus, the magnitude of the output wave $|b_0|$ due to an input wave $\mathbf{a}$ is expressed by

$$|b_0| = |\mathbf{d} \cdot \mathbf{a}| = |\eta_0|. \tag{21}$$

Combining efficiency η is then given as

$$\eta = 20 \log \frac{|b_0|}{|\mathbf{a}|} = 20 \log \frac{|\eta_0|}{\sqrt{\sum_{\nu=0}^{4N-1} |\eta_\nu|^2}} \quad [\text{dB}]. \tag{22}$$

Using the equation, numerical analysis was carried out for the combiners of optimal design. Fig. 8 shows a typical result of the analysis. At frequency f_0, the combining efficiency does not depend on the distribution among ports, when both the number of the port with phase deviation and the magnitudes of the deviations are given. When phase deviation occurs in one port, a phase margin in which the degradation of η is less than 0.1 dB is ± 20.1 deg for four-way combiner $(N = 1)$, and it increases with N. In the worst distribution of phase deviation, the phase margin is ± 10.5 deg for four-way combiner $(N = 1)$, and it decreases slightly with N. Results of the calculation based on the equivalent circuit of Fig. 3 showed that bandwidth depends little on the phase deviation within which the degradation of η remains less than 0.1 dB.

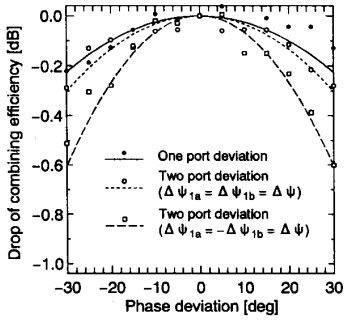

Fig. 8. Drop of combining efficiency due to phase deviation in input signals of a four-way combiner.

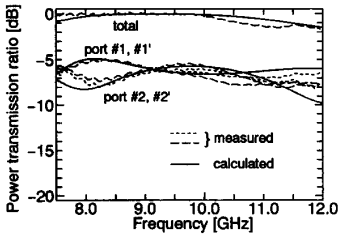

Fig. 9. Frequency characteristic of the eight-way divider ($g_p = 0.66$, $b_p = 0.54$).

TABLE II
PARAMETER VALUES OF THE DIVIDERS FOR EXPERIMENTS

	probe-pair				central probe				
N	s[mm]	d_p[mm]	g_p	jb_p	d_c[mm]	D[mm]	ϕ_c[rad]	g_c	jb_c
1	3.2	8.0	1.25	$j0.68$	4.5	10.0	1.49	0.77	$j0.24$
2	3.2	7.0	0.66	$j0.54$	4.5	10.0	1.39	0.77	$j0.24$
3	3.2	6.5	0.47	$j0.47$	4.5	10.0	1.32	0.77	$j0.24$
4	4.0	5.6	0.42	$j0.47$	4.5	9.0	1.30	0.63	$j0.26$

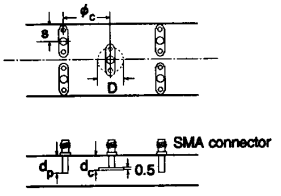

TABLE III
MEASURED CHARACTERISTICS OF THE DIVIDER

Number of ports ($4N$)	4	8	12	16
-0.5dB relative bandwidth	0.5	0.38	0.38	0.17
Insertion loss	Less than 0.1dB			

C. Frequency Characteristics of the Divider-Combiner System

Consider a series connection of a ladder divider with a ladder combiner of same structure and discuss on the characteristics of total system. There are two way of typical connection: 1) Each port of the k-th port-pair of the divider is connected to a corresponding port of the combiner (straight connection). 2) Each port of the k-th port-pair of the divider is connected to a port of the $(N - k + 1)$-th port-pair of the combiner (cross connection). In both the cases, the lengths of connecting cables must be taken to satisfy the phase relations (8) and (9). In the following, the latter case is investigated, because the lengths of the connecting cables are more uniform so that better frequency characteristics may be expected. Numerical analysis of frequency dependence of total efficiency which is defined as the ratio of output power of the combiner to input power of the divider was carried out based on the equivalent circuits of Fig. 2 and Fig. 3. Table I-C shows the maximal -0.5 dB bandwidths and corresponding probe admittances g_p and b_p under the same limitation $\phi_k \geq 1.2$ rad $(2 \leq k \leq N)$ as mentioned before. The bandwidth is smaller than that of the divider alone. The main reason is considered that, as mentioned at the beginning of this section, input phases deviate from the optimal values of (9) at frequencies other than f_0. The optimal values of g_p and b_p differ only a little from those for the divider alone. The maximal -0.5 dB relative bandwidth of the divider-combiner system is more than ten percent when the number of ports is less than twelve $(N \leq 3)$. An analysis when the dispersion of the waveguide sections of the divider/combiner is neglected shows considerable improvement of bandwidths : the relative bandwidths of the divider alone, the combiner alone and the divider-combiner system for $N = 3$ structure are respectively 0.56, 0.22 and 0.31 in no dispersion case, while they are respectively 0.43, 0.17 and 0.13 in Table I. Drops of the efficiency of dividers, combiners and divider-combiner system at frequencies other than f_0 become larger with the extent of dispersion of the waveguide.

V. EXPERIMENTS

Experiments on the double ladder-divider/combiner's were carried out for $N = 1 \sim 4$. The divider/combiner's were designed at 9.0 GHz. The design of probe-pairs whose admittances were close to the optimal values given in Table I was determined through measurement of the admittance with the probe length d_p and the position s (see the figure attached to Table II) varied. Table II shows the values of structural parameters of the divider/combiner's used in the experiments. The remaining parameters were determined using (5) $\sim$ (7) and (10). Fig. 9 shows measured frequency characteristics of the eight-way $(N = 2)$ divider together with calculated results. Table III gives measured -0.5 dB relative bandwidths for dividers of $N = 1 \sim 4$, which almost agree with the calculated results. The insertion losses at frequency f_0 (= 9.0 GHz) were less than 0.1 dB for the dividers of $N = 1 \sim 4$.

Measurements for divider-combiner systems of cross connection were also carried out. Two same structures whose parameters are given in Table II were used as both the divider and the combiner. Fig. 10 shows measured insertion loss of an eight-way $(N = 2)$ divider-combiner system in which the divider and the combiner were connected by eight coaxial cables. All the cables had the same length because, in case of

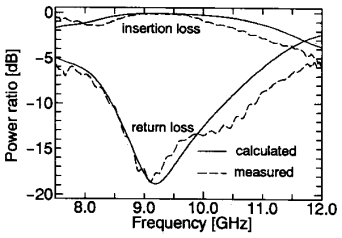

Fig. 10. Frequency characteristic of the eight-way divider-combiner system ($g_p = 0.66$, $b_p = 0.54$).

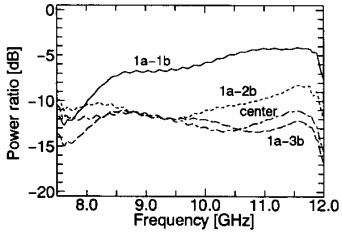

Fig. 11. Measured isolation characteristics between port #1a and the other ports ($N = 3$, $g_p = 0.66$, $b_p = 0.54$).

$N = 2$, the same length is required as derived from (8) and (9). Losses of the cables were calibrated. The results of the $N = 1$ and 2 systems gave low loss and broadband characteristics: the insertion losses were less than 0.1 dB and -0.5 dB relative bandwidths were 0.22 and 0.13, respectively.

Fig. 11 shows a typical isolation characteristics of a twelve-way divider/combiner. Measured power transmission coefficients between port #1a and the other ports are plotted in the figure (the corresponding calculated result is given in Fig. 7), where worst case isolation are shown. It is seen that the results qualitatively agree with calculated, except for two ports #1a and #1b which belong to the same port-pair, and the isolation is better than about 10 dB around the frequency f_0 except for the above two ports. The coefficients to the ports in opposite side of the central probe is smaller than -20 dB, being in good accordance with the theory. It is considered that poor accordance for the paired two ports resulted because higher waveguide modes come to affect the isolation, whereas they are not taken into account in the analysis based on the equivalent circuit of Fig. 6.

Measurements on deterioration of combining efficiency due to the phase deviation discussed in Section IV-C were carried out for a four-way combiner. The result is shown in Fig. 8 together with the calculated result, which indicates a good accordance with each other.

VI. Conclusion

We have proposed a microwave power divider/combiner of double-ladder multiple-port structure which is advantageous for its very low insertion loss and high power capability. Analysis based on equivalent circuits has given the design formula for perfect power dividing/combining.

For divider operation, numerical analysis on frequency characteristics has been carried out and the optimal design parameters for broadband characteristics has been obtained. Analysis of power flows in the structure has clarified mechanism of perfect power dividing and has shown that, under the broadband design, the divider has a quasi-traveling wave operation. The isolation characteristics of the divider has been discussed theoretically through its S-parameters.

For combiner operation, frequency characteristics have been calculated and the optimal design parameters have been also obtained. The effect of the phase deviation of input signals on the combining efficiency has been analyzed.

Experiments were carried out at X-band and the measured results indicated good performances in accordance with the theory. The -0.5 dB relative bandwidths of four-, eight- and twelve-way dividers were as large as 0.5, 0.38 and 0.38, respectively. For four- and eight-way divider-combiner systems, relative bandwidths were 0.22 and 0.13, respectively, and the insertion losses were less than 0.1 dB.

Introduction of the double-ladder structure brings remarkably broader frequency characteristics compared with the single-ladder structure of same number of ports. Even in the comparison with the latter structure with half number of ports, the former structure has broader characteristics due to the difference in the input/output port structure. As for the isolation characteristics, a satisfactory result has not been obtained yet both in the double-ladder structure and in the single-ladder structure, though isolation tends to be higher with the number of ports. Improvement of the isolation remains as a future subject. Also, graceful degradation property must be investigated, because it is important to discuss influences of failures of active devices on remaining devices and on the combiner output power. As mentioned in Section III, ladder-structure divider/combiner can exhibit a quasi-traveling wave operation which brings a wideband characteristic. Waveguide type divider/combiner's of traveling wave operation will be a next attractive subject to be studied.

Acknowledgment

The authors wish to thank Dr. M. Sanagi for valuable discussions. Thanks are also given to M. Sakuramoto for his considerable assistance in the course of experiments.

References

[1] K. J. Russell, "Microwave power combining techniques," *IEEE Trans. Microwave Theory Tech.*, vol. MTT-27, pp. 472–478, May 1970.
[2] K. Chang and C. Sun, "Millimeter-wave power combining techniques," *IEEE Trans. Microwave Theory Tech.*, vol. MTT-31, pp. 91–107, Feb. 1983.
[3] J. Goel, "A K-band GaAs FET amplifier with 8.2-W output power," *IEEE Trans. Microwave Theory Tech.*, vol. MTT-32, pp. 317–324, Mar. 1984.
[4] E. Belohoubek, R. Brown, H. Johnson, A. Fathy, D. Bechtle, D. Kalokitis *et al.*, "30-Way radial power combiner for miniature GaAs FET power amplifiers," in *1986 IEEE MTT-S Symp. Dig.*, pp. 515–518.
[5] G. Gatti, "High efficiency 4 GHz SSPA for space application," in *1986 IEEE MTT-S Symp. Digest*, pp. 319–322.
[6] N. LaParde, H. Zelen, P. Caporossi, and L. Dolan, "Ku-band SSPA for communications satellites," *American Inst. Aeronautics Astronautics*, pp. 321–325, 1986.
[7] J. Goel, G. Oransky, P. O'Sullivan, and S. Yuan, "An 8.0 watt K-band FET amplifier for satellite downlink," in *1983 IEEE MTT-S Symp. Digest*, pp. 273–375.

[8] G. W. Swift and D. Stones, "A comprehensive design techniqe for radial wave power combiner," in *1988 IEEE MTT-S Symp. Dig.*, pp. 279–281.
[9] M. E. Bialkowski and V. P. Waris, "A systematic approach to the design of radial waveguide dividers/combiners," *4th Asia-Pac. Microwave Conf. Proc.*, Adelaide, Australia, pp. 881–884, Aug. 1992.
[10] Y. Tokumitsu, T. Saito, N. Okubo, and Y. Kaneko, "A 6 GHz 80-W GaAs FET amplifier with a TM-Mode cavity power combiner," *IEEE Trans. Microwave Theory Tech.*, vol. MTT-32, pp. 301–308, Mar. 1984.
[11] H. Matsumura and H. Mizuno, "Design of microwave power combiner with circular TM_{0m0} mode cavity," *Trans. IEICE Japan*, vol. J69-C, no. 9, pp. 1140–1147, Sept. 1986.
[12] H. Matsumura, "Analysis of a microwave power amplifier using a combiner/divider with circular cavities," *IEEE Trans. Microwave Theory Tech.*, vol. 38, July 1990.
[13] K. Fukui, S. Nogi, A. Sanada, and S. Oishi, "Ladder type microwave power divider/combiner's," *Trans. IEICE Jap.*, vol. J74-C-I, pp. 27–37, Jan. 1991.
[14] E. Wilkinson, "An N-way hybrid power divider," *IRE Trans. Microwave Theory Tech*, vol. MTT-8, pp. 116–118, Jan. 1960.
[15] S.Nogi and K. Fukui, "Optimum design and performance of a microwave ladder oscillator with many diode mount pairs," *IEEE Trans. Microwave Theory Tech.*, vol. 30, pp. 735–743, May 1982.

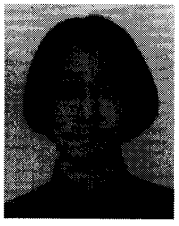

Atsushi Sanada (S'93) was born March 4, 1967 in Okayama prefecture, Japan. He received the B.E. and M.E. degrees in electronic engineering from Okayama University, Okayama, Japan, in 1989 and 1991, respectively. He is currently pursuing a D.Eng. degree at the Graduate School of Natural Science and Technology, Okayama University.

His research interests include microwave power dividing/combining.

Mr. Sanada is a member of the IEICE of Japan.

Kiyoshi Fukui (M'75) was born January 13, 1930 in Tokushima prefecture, Japan. He received the B.Sc. degree in physics in 1952 and the D.Eng. degree in electronic engineering in 1964, both from Kyoto University, Kyoto, Japan.

From 1959 to 1962, he was a Research Assistant in the Department of Electronics, Kyoto University. From 1962 to 1967, he was an Assistant professor at the Training Institute for Engineering Teachers, Kyoto University. In 1967, he be came a Professor of Electronics at Himeji Institute of Technology, Himeji, Japan. Since 1971, he has been with the Department of Electronics, Okayama University, Okayama, Japan. During the 1977–78 academic year, he was a Visiting Professor at the University of Wisconsin at Madison. His research interests have been mainly in nonlinear phenomena in electronics such as locking phenomena in oscillators, microwave power combining, and nonlinear wave propagation.

Dr. Fukui is a member of the IEICE of Japan, the Institute of Electrical Engineers of Japan, and the Physical Society of Japan.

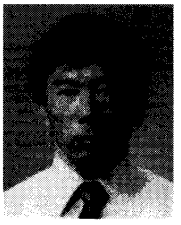

Shigeji Nogi (M'88) was born December 26, 1945, in Osaka prefecture, Japan. He received the B.E., M.E., and D.Eng. degrees in electronics from Kyoto University, Kyoto, Japan, in 1968, 1970 and 1984, respectively.

From 1970 to 1972, he was employed by the Central Research Laboratory, Mitsubishi Electric Corporation, Amagasaki, Japan. In 1972, he joined the Faculty of Engineering, Okayama University, Okayama, Japan, where he is now an Associate Professor. He spent a ten-month sabbatical leave at the University of California, Los Angeles in 1992. He has been engaged in research on microwave and millimeter-wave power combining, multimode oscillators, and nonlinear wave propagation.

Dr. Nogi is a member of the IEICE of Japan, and the Institute of Television Engineers of Japan.